Doklady Earth Sciences, Vol. 403, No. 5, 2005, pp. 812–815. Translated from Doklady Akademii Nauk, Vol. 403, No. 2, 2005, pp. 253–257.

GEOPHYSICS

Subordination of Microstructure Deformations and Brittle Macrodestructions

Yu. L. Rebetskii, R. A. Lementuyeva, N. I. D'yaur, and A. V. Mikhailova

Presented by Academician S.V. Gol'din December 24, 2004

Received December 29, 2004

The aim of our study was to distinguish the regularity of variations in the stress-and-strain state in the neighborhood of a brittle fracture at the stage preceding its appearance on the basis of laboratory experiments with rock sample breakdown. Cubic samples of limestone and sandstone, 10 x 10 cm in size, were loaded by injecting a nonexplosive destructive mixture (NDM) into a specially prepared cylindrical hole in the sample [1]. The measuring rosettes included three strain sensors pasted at an angle of 45° to each other on both horizontal and vertical planes of the sample at the exits of the tensile fracture formed during loading (Fig. 1c). Supplementing the strain sensor data on deformations ε_{xx}, ε_{yy}, and ε_{xy} on the sample plane with expressions that determine the zero stress on lateral planes of the sample allowed us to calculate all six components of the strain tensor. We studied the regularities of variations in mean strain θ, maximal shear strain γ, and in the values of the Lode–Nadai coefficient μ_ε, which determines the form of the strain tensor:

$$\theta = \frac{\varepsilon_1+\varepsilon_2+\varepsilon_3}{3}, \quad \gamma = \frac{\varepsilon_1-\varepsilon_3}{2},$$
$$\mu_e = 2\frac{\varepsilon_2-\varepsilon_3}{\varepsilon_1-\varepsilon_3} - 1. \qquad (1)$$

In Fig. 1, graphs of these parameters are shown in a dimensionless form on the time scale (the unity corresponds to the time of tensile fracture $T_{\rm tf}$ appearance at the surface) and strain scale (normalization was performed by the value of maximal shear strain at the moment of fracturing). The initial stage of loading, which is accompanied by nonlinear effects related to nonlinear increases in the NDM load and the consolidation of the sandstone or limestone structure, was not used for the analysis.

Schmidt Joint Institute of Physics of the Earth, Russian Academy of Sciences, ul. Bol'shaya Gruzinskaya 10, Moscow, 123810 Russia

We performed a preliminary theoretical analysis on the stressed state of samples for the elastic strain stage based on the results of analytical calculations and numerical modeling using the UWAY software [2]. The modeling demonstrated that coefficient μ_e changes in the sample volume from a value equal to the ratio between internal external radiuses (in our case, it was equal to 0.1, which corresponds to $\varepsilon_3 = -0.1$) near the internal surface of the pipe to –1 at the external contour. Volume deformations are equal everywhere and depend only on internal pressure. The maximal shear strains linearly depend on internal pressure and change nonlinearly in the radial direction. Deformations of maximal contraction ε_3 are formed in the pipe radius direction, while deformations of maximal extension ε_1 are formed in the tangential direction.

Rosette 1, pasted on the horizontal surface of the sample near the NDM-containing inclusion, yielded μ_e values close to –0.55 at the initial elastic stage ($0.1T_{\rm tf}$) (Fig. 1a). At this moment, intermediate main strains ε_2 are formed normal to the lateral surface (axis z), while the strain components θ and γ increase slowly and almost linearly. This stage terminates in a sharp drop of μ_e to –1, which corresponded to a reindexing of the main strain in the z axis direction ($\varepsilon_2 = \varepsilon_3 = \varepsilon_{zz}$). After reindexing, μ_e increased to +0.2, which was accompanied by a sharp increase in the slope of the graph of strain components θ and γ. This stage had a duration of 0.3 $T_{\rm tf}$ and terminated in the stabilization of the values of μ_e, θ, and γ. It is possible that at this moment the energy of the external load was used for the formation of the tensile crack surface (fracture preparation stage). The short stabilization stage ($0.05T_{\rm tf}$) gave way to a sharp drop of μ_e to zero, accompanied by a new stage of rapid increase in the values of θ and γ at the moment of macrofracture exhumation to the upper surface of the sample. The analysis of strain characteristics based on rosette 1 allowed us to distinguish three stages: (1) linear elastic deformation; (2) nonlinear deformation; and (3) preparation of the fracture and breakdown of the sample. Nonlinearity of deformation is related to the accumulation of defects in the sample interior near the cylindrical inclusion. In the course of loading, this zone

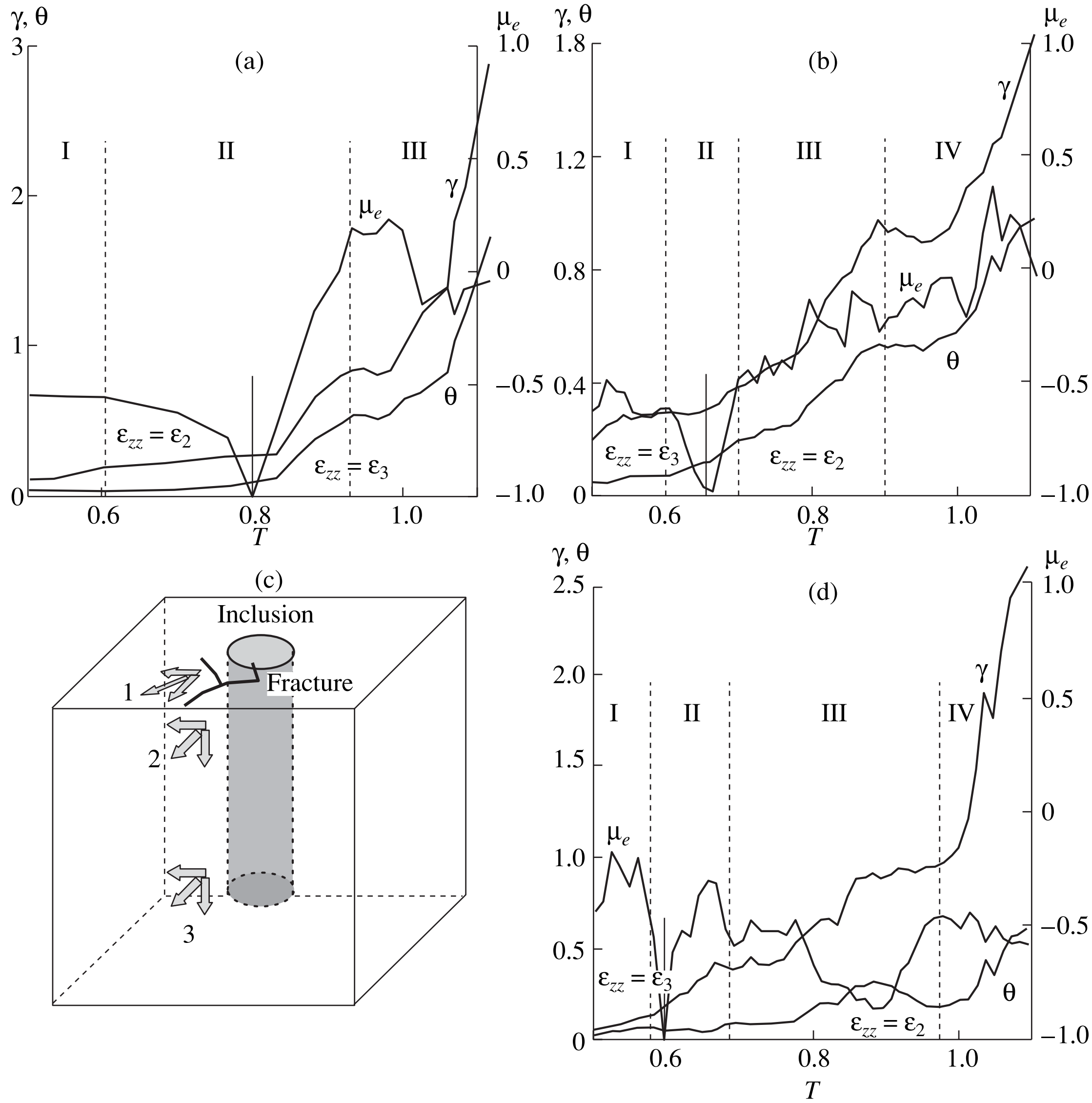

Fig. 1. (a, b, d) Variation of characteristics θ, γ, and μ_e in the sample based on the data from rosettes 1, 2, and 3 (c) Schematic location of the rosettes, position of the cylindrical inclusion with NDM, and the exhumation of tensile fracture on the horizontal surface of the sample.

gradually widened and involved zones of future tensile fracture in the nonlinear deformation stage.

Rosettes 2 and 3 were pasted on the vertical lateral surface of the sample (Figs. 1b, 1d). Since the hole in the sample for NDM filling was drilled to 4/5 of the depth, the mean μ_e values at the initial elastic stage were close to –0.6 for rosette 2, pasted in the upper part of the sample surface, and close to –0.3 for rosette 3, which was located near the bottom level of the NDM-containing cylindrical hole. In both cases, algebraically minimal deformations ε_3 are formed in the normal direction to the surface (axis z), and the increase in θ and γ values at this stage is close to linear. During the nonlinear stage determined on the basis of the analysis of rosette 1 data, the μ_e values drop to –1. At these moments, the main strain is reindexed in the direction perpendicular to the vertical surface of the sample ($\varepsilon_2 = \varepsilon_3 = \varepsilon_{zz}$), after which intermediate main strains ε_2 are formed in this direction. At first, the reindexing occurs at rosette 3. As in rosette 1, the reindexing in rosette 2 after some delay is caused by the nonlinearity of the strain developing from the NDM-containing cylindrical inclusion in the sample interior.

The reindexing is followed by an increase in the slope of θ and γ graphs (except for θ at rosette 3), a rapid increase in μ_e to –0.5, and the commencement of the stabilization stage. It is likely that the nonlinearity in the strain parameter graphs for rosettes 2 and 3 of this stage is caused by the development of the nonlinear deformation segment near the inclusion. The stabilization stage μ_e is followed by a new increase in the slope of θ and γ graphs. It is possible that the increase in strains is related to the appearance of a tensile fracture in the sample interior near the NDM-containing cylindrical inclusion and to the expansion of zones involved in nonlinear deformation up to the vertical surface. In this case, the μ_e value increases to –0.2 for rosette 2 and decreases to –0.8 for rosette 3. The last stage of increase in the slope of θ and γ graphs is related to the exhumation of the tensile fracture. Thus, the analysis of strain characteristics based on rosettes 2 and 3 allowed us to distinguish four stages: (1) linear elastic deformation; (2) nonlinear deformation near the inclusion; (3) the appearance of the tensile fracture near the inclusion and nonlinear deformation near the vertical surface; and (4) preparation of the fracture and its appearance near the vertical surface of the sample.

Taken together, the analytical and numerical modeling results correspond well to the data obtained in the experiments using strain sensors at the initial elastic stage. At the same time, UWAY-based calculations did not yield any variations in the parameters of the stress-and-strain state such as were observed in the experiments at the brittle fracture stage (we considered a linearly elastic model with the tensile fracture growing from one of the planes). The experimental result may be related to the following fact: samples subjected to brittle deformation are marked by a stage in which defects accumulate in the nonlinear deformation zone, and this stage was absent in the numerical modeling.

Indirect data on the nature of the process at the nonlinear deformation stage were also obtained on the basis of electric potential (EP) and ultrasound profiling (USP) data [1]. It was found that this stage is characterized by an increase in the EP growth rate, and its variation mode is similar to that of variations in the mean deformation θ. Initially, the EP growth rate is small, but later it begins to increase sharply. One can see a certain advance in the EP variation relative to the θ variation. The USP-based elastic wave velocities remain virtually constant for a long period (the EP value at this stage is already 50% higher relative to the linear deformation stage) and they sharply decrease only immediately prior to the appearance of a macrofracture.

Comprehensive analysis of the results of our experiments and data reported in [3] allowed us to make a supposition concerning the peculiarities of the microstructure transformations that precede brittle destruction and that are reflected as variations in strain characteristics. The microstructural transformations, which occur in very narrow zones at the nonlinear deformation stage, most likely generate an echelon of microshears and subordinate microfractures. They are oriented in accordance with the Coulomb theory of strength and lead to the partial removal of elastic deformations in the direction of two main (algebraically maximal and minimal) strain axes, which are replenished owing to the continued loading. In turn, microfractures accompanying the appearance of microshears decrease the effective tensile strength. On the whole, microstructural transformations can be defined as plastic deformations, the appearance and development of which decrease the strength. Such microstructural transformations lead to a decrease in the energy spent on destruction.

It is noteworthy that the performed experiments were characterized by some peculiarities, owing to which it is not possible to estimate their results from the standpoint of the classic mechanics of brittle destruction. In particular, the loading rate appeared to be small relative to the microdestruction rate. Therefore, the plastic deformation zone is more extended than the characteristic dimensions of the model. Thus, the properties of the microfracture formation zone differ from those of the environment. Therefore, one cannot say that the growth rate of the deformation zone is related only to the coefficient of stresses in the crack mouth. Under such conditions, the growth rate of macrofractures and the critical parameters of growth stages will be related not only to the loading mechanism, but also to the rate of structural transformations. At certain moments of time, the energy accumulated in microstructures (internal stresses) can be sufficient for the growth of a macrofracture even after the termination of further loading.

Let us analyze some possible variations in the deformation regime of the future brittle fracture zone at the microstructural transformation stage for a point on the sample surface near the inclusion (comparison with the data on rosette 1). This zone is marked by plastic unloading owing to shear displacements along the Coulomb–Moore microfractures, which are formed along the shear planes. The development of microdisplacements leads to a decrease in the level of maximal shear stress in the radial direction by $\Delta\sigma$. Owing to a decrease in the intensity of radial compression (given that the level of other main stresses is retained), elastic deformations are redistributed along the axes of the main stresses. If we consider that the orientation of the main axes of stress does not change at these transformations (the cleavage plane is close to the plane of maximal tangent stresses τ_{13}), then the increments of elastic deformations in the maximal shear deformation will be equal to the increments of the residual (plastic) shear deformations. It is possible to show that in this case the values of the parameters under study would be determined by the following relations:

$$\mu_e = \mu_e^0 - \kappa\frac{\Delta\sigma}{\gamma^0}, \qquad \theta = \theta^0 + \lambda\Delta\sigma, \quad \gamma = \gamma^0, \tag{2}$$

where κ and λ are elastic constants depending on the elastic modulus and Poisson coefficient, and the upper index equal to zero denotes the value of the respective parameters before the appearance of a microshear deformation. As seen from relations (2), the value of coefficient μ_e at the microstructural transformation stage should be close to –1 (uniaxial elongation). Reindexing of the axes of main deformations occurs when the deformed state corresponds to uniaxial elongation. At this point, deformations ε_3 are formed at the analyzed macropoint in the direction z perpendicular to the sample surface.

After equalizing the main elastic deformations with indices 2 and 3, further removal of elastic deformations may occur due to both displacements along microshears in the planes perpendicular to the horizontal surface and displacements along new microshears, whose planes are inclined at an angle of 45° to the z axis and tangential direction (plane of action τ_{12} before reindexing). In this case, the form of the stress tensor should always remain close to uniaxial extension ($\mu_e \approx -1$). However, this is not observed in the experiment. Here, strains ε_3 are formed in the z axis direction after reindexing and up to the point of destruction. This situation is possible if we suppose that microshears formed at the previous stage changed strength properties of the medium. The old microshears lock the zone and hamper the formation of microshears in other directions (anisotropy of strength). After reindexing of the axes of main deformations, the accumulation of residual strains and release of elastic energy continues owing to microshears formed in the plane of tangential stresses τ_{12} (plane τ_{13} before reindexing). This stage is marked by an increase in the maximal tangential stress τ_{13} up to the critical value. This is followed by an avalanche formation of microshears and hierarchic microfractures in the plane of tangential stress τ_{13} action. At this stage, zones of higher dilatancy and lower strength are developed in the structural rearrangement zone owing to the formation of two conjugated systems of fractures and cleavages. The widening and merging of such zones is the last occurrence in the microstructural rearrangement before the formation of tensile macrofracture.

The results of our experiments make it possible to explain the nature of regular variations in the tectonic stresses revealed by tectonophysical reconstruction. For example, a reconstruction of the modern stressed state of the Kuril–Kamchatka seismoactive zone using data on earthquake focus mechanisms [4] allowed us to distinguish periodic variations accompanied by a sign change in the Lode–Nadai coefficient. Strong earthquakes ($M_b > 7.5$) are always preceded by a decreased μ_σ stage, whose duration is related to the magnitude of the event, whereas the earthquake itself occurs at the stage of μ_σ growth. Reconstruction of paleostresses based on the shear fracture data [5] at magmatic, hydrothermal, and hydrothermal-metasomatic deposits demonstrated that ore bodies are usually confined to rock zones that are characterized by a high variability in the orientation of the main stress axes and by the widest range of μ_σ variations.

ACKNOWLEDGMENTS

This work was supported by the Russian Foundation for Basic Research, projects nos. 03-05-64709, 03-05-64998, and 03-05-65092.

REFERENCES

1. G. A. Sobolev, R. A. Lementueva, and A. A. Gvozdev, in *Modeling of Geophysical Processes* (OIFZ RAN, Moscow, 2003), pp. 5–9 [in Russian].
2. A. N. Vlasov, M. G. Mnushkin, and Yu. G. Yanovsky, *Proceedings EPMESC VIII International Conference in Enhancement and Promotion of Computational Methods in Engineering and Science, Shanghai, July 25–28, 2001* (Shanghai San Lian Publ., Shanghai, 2001), pp. 280–281.
3. A. N. Stavrogin and A. G. Protosenya, *Mechanics of Deformation and Breakdown of Rocks* (Nedra, Moscow, 1992) [in Russian].
4. O. I. Gushchenko, in *Nature and Methodology of Determination of Tectonic Stresses in the Upper Section of the Earth's Crust* (Apatity, 1987), pp. 35–52 [in Russian].
5. L. A. Sim, N. Yu. Vasil'ev, V. A. Korchemagin, and V. S. Emets, in *Stress and Strain Fields in the Earth's Crust* (Nauka, Moscow, 1987), pp. 159–163 [in Russian].